Structural and Thermodynamic Characteristics of cHLH Peptide and cHLH/HDM2 Complex

Haeri Im, Sunhee Cho, and Sihyun Ham*

Department of Chemistry, Sookmyung Women's University, Cheongpa-ro 47-gill 100, Yongsan-gu, Seoul, 04310, Korea.

Tumor suppressor protein p53 loses its function upon binding with the HDM2 protein, and inhibiting the p53-HDM2 interaction is critical to suppress tumor cell growth. Recently, the cyclized helix-loop-helix peptide (cHLH) mimicking the α-helix part of the p53 protein has been designed and found to exhibit high binding affinity with HDM2. Here, we report the structural and thermodynamic characteristics of the bound complex of the cHLH peptide with the HDM2 protein. We performed molecular dynamics simulations to investigate the structural features of the cHLH peptide as well as its complex with the HDM2. The binding free energy calculation based on the integral equation theory was also executed to quantify the binding affinity for the cHLH/HDM2 complex and to understand the factors contributing to the binding affinity. We found a variety of factors for the helix stability of the cHLH peptide as well as in the complexation with the HDM2, which may provide an insight into the development of anti-cancer drug designs.

Keywords: Cyclized Helix-Loop-Helix, Protein-Protein Interaction, Molecular Dynamics Simulations, Solvation Free Energy

Introduction

Tumor suppressor protein p53 controls the cell cycle arrest, apoptosis, and DNA repair from the stress signals.[1-3] Loss of the p53 function is a common feature in the majority of human cancer.[4-6] Also inactivation of the p53 tumor suppressor by the HDM2 is one of the most frequent events in cancer.[7] Therefore, the HDM2 is related to a variety of human cancers, and compound targeting the p53/HDM2 interaction are promising for cancer therapy.[7,8] In the previous studies, protein-protein interaction (PPI) was a significant part of the targeted anticancer therapy and it was studied about drug discovery.[9] Some structures were mimicked epitope residues in the p53 to inhibit of interaction between the p53 and the HDM2.[10,11] Also binding site in the p53/HDM2 complex was investigated. F19, W23, and L26 in the helix of the p53 were determined epitope residues in the p53/HDM2 complex.[12]

Here we report the structural and thermodynamic characteristics of the cyclized helix-loop-helix peptide (cHLH) and the cHLH/HDM2 complex by using all-atom, explicit water molecular dynamics (MD) simulations as well as three-dimensional reference interaction site model (3D-RISM) theory. Firstly, we investigate structural features of structures (cHLH peptide and cHLH/HDM2 complex), and observe factors relevant to the structural stability. Secondly, we elucidate the importance of solvation effect in in the complex formation.

Theory and Computational Method

1. Molecular Dynamics Simulations

We carried out all-atom, explicit-water MD simulation at 300 K and 1 bar on the cHLH peptide and the cHLH/HDM2 complex by using PMEMD-cuda module of AMBER 14 package.[13] We employed the ff99SB-ILDN force field[14] for protein and TIP3P model[15] for water. The cHLH/HDM2 complex structure was made by using AutoDock 4.0[16]. The SHAKE algorithm[17] was employed for bond including hydrogen atoms. Production runs of the cHLH peptide and the cHLH/HDM2 complex were conducted for 50 ns and 10 ns under neutral pH, respectively. Particle mesh Ewald method[18] was applied for treating long-range electrostatic interactions, while a 12 Å cut-off was used for the short-range non-bonded interactions.

2. Solvation Free Energy Analysis

For protein conformation generated by the MD simulation, we calculated the three-dimensional reference interaction site model (3D-RISM) theory[19,20] for solvation free energy. The 3D-RISM theory is an integral-equation theory based on

statistical mechanics for obtaining the 3D distribution function $g_i(r) = h_i(r) + 1$ of the water site i position r around a protein. In this theory, the 3D-RISM equation

$$h_i(r) = \sum_j \int dr' \chi_{ij}(|r - r'|)c_j(r')$$

Is solved self-consistently with the closure relation

$$h_i(\mathrm{r}) = \begin{cases} \exp[-\beta u_i(r) + h_i(r) - c_i(r)] - 1 & \text{for } h_i(r) \le 0 \\ -\beta u_i(r) + h_i(r) - c_i(r) & \text{for } h_\gamma(r) > 0 \end{cases}$$

In these equations, $c_i(r)$ is the direct correlation function, $\chi_{ij}(r)$ is the water susceptibility function, $u_i(r)$ is the protein-water interaction potential, and $\beta = 1/(k_B T)$ is the inverse temperature. The solvation free energy G_{solv} is obtained from

$$G_{solv} = \rho k_B T \sum_i \int dr \left[\frac{1}{2} h_i(r)^2 \Theta\big(h_i(r)\big) - c_i(r) - \frac{1}{2} h_i(r) c_i(r)\right]$$

Where ρ is the average number density of water and $\Theta(x)$ is the Heaviside step function.

Results and Discussion

Structural Characteristics of cHLH Peptide

The cHLH peptide was designed to mimic the p53 and epitope residues are grafted in the cHLH helix 2 (Figure 1). To understand the structural characteristics of the cHLH peptide by performing the MD simulations, we first analyzed the structural features. The Cα root-mean-square deviation (RMSD) values are relatively low with the average of 3.3 Å (standard deviation: 0.7 Å). The distribution of radius of gyration (Rg) is fairy restricted (data not shown) with the average value of 10.2 Å (0.1 Å). The distribution of Cα root-mean-square fluctuation (RMSF) is shown in Figure 2. The helix 1 and helix 2 regions exhibit less fluctuations compared to the loop region. The averaged secondary structural data are shown in Figure 3. The averaged helicity (61%) of the entire structure during the simulations is considerably high. In the more details, based on the residue-specific secondary structure calculations, high helical character on the entire helices sequence (residues 2-16 and 24-38) is indicated, whereas the thioether bond and loop region are indicated less than that of the helix region. The high helical character of the cHLH peptide mainly arises from the salt-bridge formation on the helix 1 and hydrophobic interactions on the helix 2. Firstly, salt-bridge formation on the helix 1 is important to maintain the helical character of the cHLH peptide. The six grafted arginine residues (R3, R6, R7, R10, R13, and R14) interact with four

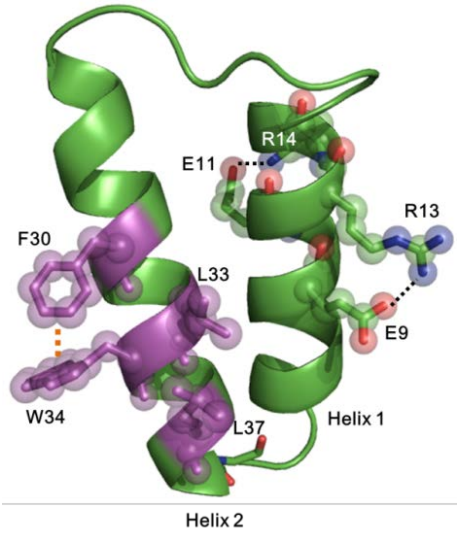

Figure 1. Representative cHLH peptide structure. The helix 1 region (residues 2–16) is grafted arginine residues (shown as stick representation). Also salt-bridges exist in the helix 1 region (dotted black line). The helix 2 region (residues 24–38) is grafted epitope residues (magenta-colored stick). Additionally, π-π stacking interaction exists in the helix 2 region (dotted orange line).glutamic acid residues (E4, E9, E11, and E16) through electrostatic interaction. During the simulation, salt-bridges between R6 and E9, E9 and R13, R7 and E11, and E11 and R14 are mainly conserved at the averaged level of 57 %. Secondly, grafted epitopes residues (F30, L33, W34, and L37) of the helix 2 interact with each other to form hydrophobic interactions. N-H group and C=O group in the back-bone of the alpha helix 2 interact to form hydrogen bonds, at the same time, the side-chain of grafted hydrophobic residues also interact to make hydrophobic interaction (Figure 1).

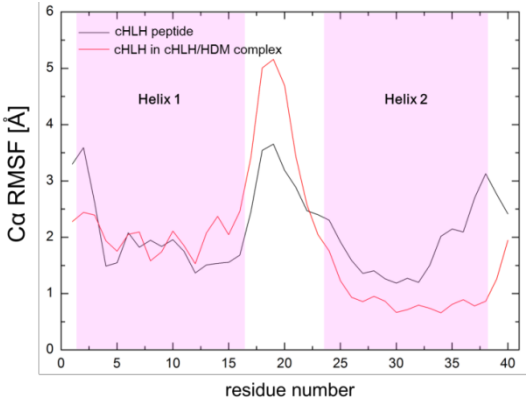

Figure 2. Backbone Cα RMSFs of the cHLH residues. Black line refers to the result for the cHLH peptide, whereas red line to that in the cHLH/HDM2 complex.

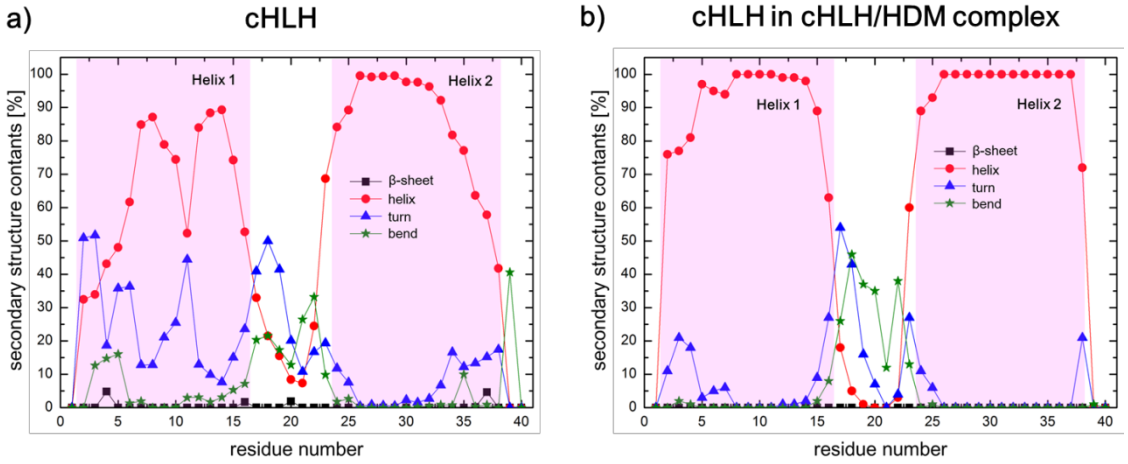

Figure 3. Average secondary structure contents of each amino acid residue for (a) The cHLH peptide and (b) The cHLH peptide in the cHLH/HDM2 complex. (Pink regions: helix 1 and helix 2, black squares: β-sheet, red circles: helix, blue triangles: turn, green stars: bend)

Especially, for F30 and W34, they interact each other to make T-shaped π-π stacking interactions. The T-shaped interaction between F30 and W34 is largely conserved during the simulation time (data not shown). The hydrophobic interactions of side-chain make helix 2 rigid not to denature alpha helical conformations. These factors, salt-bridge formation and hydrophobic interactions, contribute to the structural stability and helicity of the cHLH peptide.

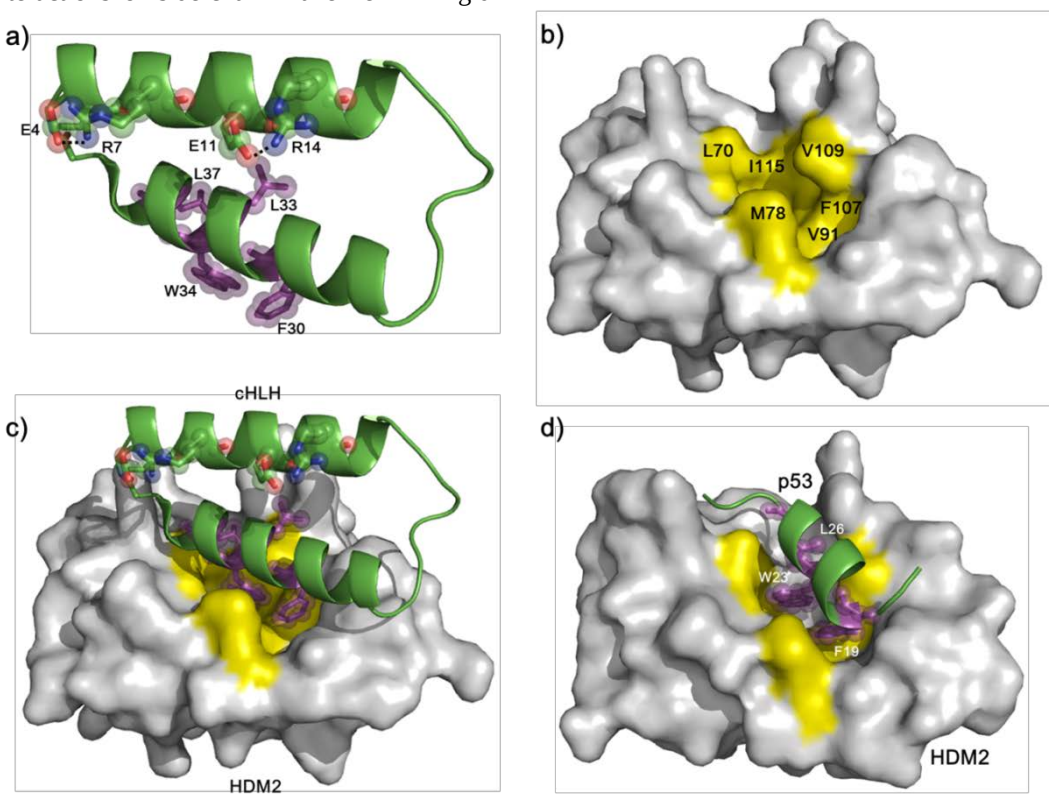

Figure 4. a) The cHLH peptide has salt-bridge and epitope residues b) The HDM2 structure surface. c) The cHLH complex with the HDM2. The epitope residues are inserted into the cleft. d) It is X-Ray structure of the p53 complex with the HDM2. (Epitope residues are magenta-colored stick. Salt-bridges between glutamic acid and arginine are dotted black line. The yellow color surface in the HDM2 indicates region of hydrophobic interaction with epitope residues of the cHLH or the p53)

Structural Characteristics of cHLH Peptide and HDM2 Complex

To understand the complex structure of the cHLH peptide bound to the HDM2, we performed molecular docking research to investigate protein binding site and 10 ns MD simulations. Firstly, when the cHLH peptide is bound to the HDM2, averaged Cα RMSFs of the helix 2 is decreased from 1.8 Å to 0.9 Å (Figure 2). This indicates that the helicity and structure stability is increased in the cHLH/HDM2 complex. Furthermore, we detected that the helicity and structure stability of the cHLH peptide in the cHLH/HDM2 complex were increased compared to those of the cHLH peptide. The number of averaged hydrogen bond in the helix 1 and helix2 was increased from 4 to 5 and from 7 to 9, respectively. Averaged helicity in the helix 2 was increased from 85 % to 97 % as well as that in the helix 1 was increased from 66 % and 91 % (Figure 3). Secondly, according to the ref. 12, F19, W23, and L26 in the p53 peptide were detected epitope residues. In the native structure of the p53 complex with the HDM2, the position of F19, W23, and L26 in the p53 helix allowed to insert deep inside the HDM2 cleft (Figure 4d). Epitope residues are hydrophobic contacted with the HDM2. Residues of hydrophobic interaction with epitope residues in the HDM2 are L54, L56, I61, M62, V75, and V93. Topology of epitope residues (F30, L33, W34, and L37) on the cHLH peptide (Figure 4a) in the cHLH/HDM2 complex was alike to topology of epitope residues on the p53 peptide in the p53/HDM2 complex (Figure 4c). We observed that epitope residues in the HDM2 had hydrophobic interaction with the HDM2. Averaged residues of hydrophobic interaction with the cHLH peptide in the HDM2 for 10 ns are L70, L73, I77, M78, L82, I90, V91, F107, V109, and I115 in the HDM2 (Figure 4b). These results indicate that cHLH bound to the HDM2 at accurate binding site in the HDM2 and cHLH peptide in the cHLH/HDM2 complex has higher helicity than that of the cHLH peptide by effect factors.

Thermodynamic Characteristics of cHLH Peptide and HDM2 Complex

To characterize the binding affinity for the complexation of the cHLH peptide and HDM2, we computed thermodynamic quantity such as internal energy (E_u), hydration free energy (G_{solv}), and effective binding free energy (f). In the gas phase, complexation of the cHLH peptide and HDM2 is not possible due to their total charge. The total charge of the cHLH peptide is +6 and that of the HDM2 is +5. Because of the repulsive force between two positively charged proteins, two proteins would not approach each other. Indeed, the computed binding energy in the gas phase (ΔE_u = +270.1 kcal/mol) is highly repulsive. However, two positively charged proteins approach each other in the aqueous environment. This is because of the water surrounding the protein. The water molecules around the protein reduce the repulsive force. The binding solvation free energy (ΔG_{solv}) is calculated as -395.6 kcal/mol. We then calculate the effective binding free energy of the cHLH peptide with the HDM2 complex and it is -125.5 kcal/mol in aqueous phase (Table 1). From this, we observed that, in the water environment, two positively charged proteins are thermodynamically like to approach.

Conclusion

We investigated the computational studies on the structural and thermodynamic characteristics of the cHLH peptide and cHLH/HDM2 complex. The binding structure and binding affinity of the cHLH/HDM2 complex were also studied to understand the molecular insight into the complexation of the p53 and HDM2. We focused on the structural stability through the helical properties of the cHLH peptide and binding affinity through the thermodynamic analysis of the cHLH/HDM2 complex. We find that the role of the salt-bridges and hydrophobic interactions including the T-shaped π-π stacking in the stabilizing the helix structure of the cHLH peptide and the hydrophobic interactions upon the complexation of the cHLH peptide and HDM2. These features are cyclized-peptide-dependent, partially experimentally measured, it is suggested that (i) salt-bridge formation, (ii) hydrophobic interaction including the T-shaped π-π stacking, (iii) hydrophobic interaction upon complexation, and (iv) effective binding free energy upon complexation, are the structural and thermodynamic

Table 1. Thermodynamic quantity of the cHLH peptide with the HDM2 complex (unit: kcal/mol). Internal energy (E_u), solvation free energy (G_{solv}), effective energy (f) = E_u + G_{solv} and their difference (Δ) = complex – (cHLH peptide + HDM2) are calculated. (Δf: effective binding free energy)

	complex	cHLH	HDM2	Difference (Δ)
E_u	-839.4	-428.2	-681.2	270.1
G_{solv}	137.3	-135.7	668.6	-395.6
f	-702.1	-563.9	-12.7	-125.5

characteristics of the cHLH peptide and cHLH/HDM2 complex. We believe that our results will serve to understand the molecular insights into the development of anti-cancer drug designs at the atomic-level

Acknowledgments. This work has been supported by the project EDISON (EDucation-research Integration through Simulation On the Net), Chemistry.

References

1. Walker, Kristen K.; Levine, Arnold J., *Proceedings of the National Academy of Sciences*, **1996**, *93*, 15335.
2. Amaral, Joana D., et al., *Journal of Biological Chemistry*, **2007**, *282*, 34250.
3. Harris, Sandra L.; Levine, Arnold J., *Oncogene*, **2005**, *24*, 2899.
4. Vogelstein, B.; Lane, D.; Levine, A. J., *Nature*, **2000**, *408*, 307.
5. Brown, C. J.; Lain, S.; Verma, C. S.; Fersht, A. R.; Lane, D. P., *Nat. Rev. Cancer*, **2009**, *9*, 862.
6. Lane, D. P.; Hupp, T. R., *Drug Discovery Today*, **2003**, *8*, 347.
7. Wanzel, Michael, et al., *Nature chemical biology*, **2015**, *12*, 22.
8. Onel, Kenan; Cordon-Cardo, Carlos., *Molecular Cancer Research*, **2004**, *2*, 1.
9. Hoggard, Logan R., et al., *Journal of the American Chemical Society*, **2015**, *137*, 12249.
10. Plante, Jeffrey P., et al., *Chemical Communications*, **2009**, *34*:, 5091.
11. Barnard, Anna, et al., *Angewandte Chemie International Edition*, **2015**, *54*, 2960.
12. Kussie, Paul H., et al., *Science*, **1996**, *274*, 948.
13. Case, D. A., et al. AMBER 14, *University of California, San Francisco*, **2014**.
14. Lindorff-Larsen, Kresten, et al., *Proteins: Structure, Function, and Bioinformatics*, **2010**, *78*, 1950.
15. Jorgensen, William L., et al., *The Journal of chemical physics*, **1983**, *79*, 926.
16. Trott, Oleg; Olson, Arthur J., *Journal of computational chemistry*, **2010**, *31*, 455.
17. Ryckaert, Jean-Paul; Cissotti, Giovanni; Berendsen, Herman JC., *Journal of Computational Physics*, **1977**, *23*, 327.
18. Darden, Tom; York, Darrin; Pedersen, Lee., *The Journal of chemical physics*, **1993**, *98*, 10089.
19. Kovalenko, A.; Hirata, F. Molecular Theory of Solvation. *by Hirata F., Kluwer, Dordrecht*, **2003**, 169.
20. Imai, T.; Harano, Y.; Kinoshita, M.; Kovalenko, A.; Hirata, F. *The Journal of chemical physics*, **2006**, 125.